Published in final edited form as:
Clin Exp Metastasis. 2013 June ; 30(5): 579–594. doi:10.1007/s10585-012-9562-5.

Inhibition of focal adhesion kinase (FAK) activity prevents anchorage-independent ovarian carcinoma cell growth and tumor progression

Kristy K. Ward[1,*], **Isabelle Tancioni**[1,*], **Christine Lawson**[1], **Nichol L.G. Miller**[1], **Christine Jean**[1], **Xiao Lei Chen**[1], **Sean Uryu**[1], **Josephine Kim**[1], **David Tarin**[2], **Dwayne G. Stupack**[1], **Steven C. Plaxe**[1], and **David D. Schlaepfer**[1,3]

[1]Department of Reproductive Medicine, Moores UCSD Cancer Center, La Jolla, CA 92093

[2]Department of Pathology, Moores UCSD Cancer Center, La Jolla, CA 92093

Abstract

Recurrence and spread of ovarian cancer is the 5th leading cause of death for women in the United States. Focal adhesion kinase (FAK) is a cytoplasmic protein-tyrosine kinase located on chromosome 8q24.3 (gene is *Ptk2*), a site commonly amplified in serous ovarian cancer. Elevated FAK mRNA levels in serous ovarian carcinoma are associated with decreased (logrank $P = 0.0007$, hazard ratio 1.43) patient overall survival, but how FAK functions in tumor progression remains undefined. We have isolated aggressive ovarian carcinoma cells termed ID8-IP after intraperitoneal (IP) growth of murine ID8 cells in C57Bl6 mice. Upon orthotopic implantation within the periovarian bursa space, ID8-IP cells exhibit greater tumor growth, local and distant metastasis, and elevated numbers of ascites-associated cells compared to parental ID8 cells. ID8-IP cells exhibit enhanced growth under non-adherent conditions with elevated FAK and c-Src tyrosine kinase activation compared to parental ID8 cells. In vitro, the small molecule FAK inhibitor (Pfizer, PF562,271, PF-271) at 0.1 uM selectively prevented anchorage-independent ID8-IP cell growth with the inhibition of FAK tyrosine (Y)397 but not c-Src Y416 phosphorylation. Oral PF-271 administration (30 mg/kg, twice daily) blocked FAK but not c-Src tyrosine phosphorylation in ID8-IP tumors. This was associated with decreased tumor size, prevention of peritoneal metastasis, reduced tumor-associated endothelial cell number, and increased tumor cell-associated apoptosis. FAK knockdown and re-expression assays showed that FAK activity selectively promoted anchorage-independent ID8-IP cell survival. These results support the continued evaluation of FAK inhibitors as a promising clinical treatment for ovarian cancer.

Keywords

ovarian cancer; focal adhesion kinase; cell survival; anchorage-independent cell growth; orthotopic tumor growth; metastasis; syngeneic tumor model

[3]Address correspondence to: David D. Schlaepfer, Ph.D. University of California San Diego, Moores Cancer Center Department of Reproductive Medicine, 0803 3855 Health Sciences Dr. La Jolla, CA 92093 dschlaepfer@ucsd.edu.
[*]Authors contributed equally to this study

The authors declare that they have no conflict of interest.

Introduction

Epithelial ovarian carcinoma ranks 9th among invasive malignancies diagnosed in US women in 2012 and it is the 5th leading cause of cancer death. Over 22,000 women will be diagnosed this year and over 15,000 will die from the disease [1]. First line chemotherapy with carboplatin and paclitaxel is very effective with an 80% response rate; however, 70% of those patients who respond to initial therapy will eventually recur [2,3]. Most with recurrence will die of their disease secondary to the development of tumor chemo-resistance [4].

Epithelial tumors are the most common type of ovarian cancer [5]. Unlike most other human malignancies, ovarian cancer primarily disseminates by exfoliative mechanisms. Cells dissociate from the primary tumor and can continue to survive as multi-cellular spheroids within the peritoneal space and re-implant to form new tumors on the peritoneal surface [6]. As such, the majority of epithelial ovarian cancers present with advanced disease with diffuse intra-abdominal spread [7,8]. Understanding the mechanism by which these spheroids can survive and proliferate is vital in the development of targeted therapies for this disease.

Focal adhesion kinase (FAK) is canonically thought of as cytoplasmic protein-tyrosine kinase that associates with integrins and growth factor receptors and acts to regulate various intracellular signaling pathways associated with tumor progression [9,10]. However, under conditions of FAK inhibition, FAK localizes to the cell nucleus whereby it can modulate gene expression and cell survival [11,12]. The gene for FAK (termed *Ptk2*) is located at the tip of chromosome 8q24.3 which is an ovarian cancer susceptibility locus and a site commonly amplified in ovarian cancer [13,14]. FAK protein is elevated in serous ovarian tumors compared to normal ovary [15] and women with higher FAK expression in tumors exhibit high levels of metastasis and decreased overall survival [16]. Short-interfering RNA knockdown approaches to reduce FAK expression can increase ovarian cancer apoptosis and decrease tumor size in mouse models [17,18]. In combination with Src-family tyrosine kinases, FAK is implicated in promoting adrenergic receptor-stimulated ovarian carcinoma cell survival [19]. However, as Src inhibitors such as dasatinib did not show single agent activity in patients with recurring epithelial ovarian cancer [20], it is possible that FAK signaling connections may be distinct from Src in promoting ovarian tumor progression.

Small molecules that act as ATP-competitive inhibitors of FAK activity are in various stages of development [21-24]. Completed Phase I human studies of PF-562,271 (PF-271) are encouraging as oral administration of this FAK inhibitor is tolerable and was associated with prolonged stable disease by 12% of patients [25]. Studies in human xenograft or syngeneic mouse tumor models have associated PF-271 administration with the inhibition of breast [26,27], liver [28], prostate [29,30], pancreatic [31], and squamous cell [32] tumor progression. However, the proposed mechanism(s) of action associated with FAK inhibition are varied and may also involve alterations in the tumor microenvironment [33]. Previous studies using a FAK inhibitor from Novartis (TAE-226) or Poniard (PND-1186) revealed an inhibition of ovarian carcinoma tumor growth [22,23], but whether this reflects a direct inhibition of FAK activity remains undetermined. Moreover, PF-271 effects on ovarian carcinoma cells are unknown.

Here, we have isolated an aggressive population of ID8 murine ovarian carcinoma cells after intraperitoneal (IP) growth in C57Bl6 mice (ID8-IP cells) that exhibit enhanced growth under anchorage-independent conditions and tumor metastasis in mice. ID8-IP growth in vitro and in vivo is sensitive to PF-271-mediated FAK inhibition whereby PF-271 functions to selectively block FAK but not c-Src tyrosine phosphorylation. Pharmacological FAK

inhibition also prevents the growth of various human ovarian carcinoma cells under anchorage-independent conditions. In ID8-IP cells, genetic knockdown and cell reconstitution assays show that anchorage-independent survival is dependent upon FAK expression and activity. Together, these results support the continued evaluation of FAK inhibitors as a new therapeutic treatment option for ovarian cancer.

Materials and Methods

Antibodies and reagents

Site and phospho-specific antibodies pY397 FAK (clone 141-9) and pY416 c-Src (2101) were from Life technologies and Cell Signaling, respectively. Antibodies to FAK (clone 4.47, Millipore), c-Src (sc-18, Santa Cruz Biotechnology), E-cadherin (clone 36, Life Technologies), CD31 (clone MEC13.3 BD Pharmingen), and β-actin (clone AC-74, Sigma) antibodies were purchased. PF-562,271 (PF-271) was synthesized as described [21] and PND-1186 was from Poniard. For in vitro studies, PF-271 and PND-1186 were dissolved in dimethyl sulfoxide (DMSO) and stored at -80°C until time of use. Final experimental DMSO concentration did not exceed 0.1%. For in vivo tumor experiments, oral PF-271 (30 mg/kg) or PND-1186 (150 mg/kg) administration was twice daily by gavage starting 7 days after tumor cell injection. The vehicle for PF-271 was 30% 2-hydroxypropyl-beta-cyclodextrin in 3% dextrose and the vehicle for PND-1186 was water.

Cells

Human ovarian cancer cell lines IGROV1, SKOV3, HEY, and A2780 were from J. Chien (Mayo Clinic, Rochester, MN), 2008 cells were from S. Howell (UCSD), and murine ovarian ID8 carcinoma cells were from K. Roby [34] at the Kansas University Medical Center. All cells were cultured in Dulbecco's modified Eagle's medium supplemented with 10% fetal bovine serum (FBS), 1 mM non-essential amino acids, 2 mM glutamine, 100 U/ml penicillin, and 100 μg/ml streptomycin. ID8 cells were injected into the intraperitoneal cavity of C57Bl6 mice, ascites-associated cells isolated after 45 days as described [23], and a population of ID8-IP cells was obtained and expanded by culture under anchorage-independent conditions on low binding poly 2-hydroxyethyl methacrylate (poly-HEMA) coated plates for 3-4 weeks. ID8-IP cells were stored frozen as a low passage stock and for experiments, cultured under adherent or suspended conditions for less than 6 passages.

Cloning and lentiviral constructs

The coding sequence for fluorescent mCherry protein (pmCherry-C1, Clontech) was subcloned into the lentiviral expression vector (pCDH-CMV-MSC1, System Biosciences) and recombinant lentivirus produced as described [11]. Lentivirustransduced mCherry-expressing ID8 and ID8-IP cells were selected by growth in puromycin (2 μg/ml), expanded, and frozen as low passage stocks. Short-hairpin RNA (shRNA) expression from pLentiLox 3.7-Puro (subcloning was used to replace GFP with puromycin selectable marker) was used to knockdown FAK using forward (5'-tgaagggatcagttacctgattcaagagatcaggtaactgatcccttctttttttc-3') and reverse (5'-tcgagaaaaaagaagggatcagttacctgatctcttgaatcaggtaactgatcccttca-3') targeting sequences coding for murine FAK residues (278-284). A scrambled (Scr) shRNA using forward (5'-tgtctccgaacgtgtcacgtttcaagagaacgtgacacgttcggagacttttttc-3') and reverse (5'-tcgagaaaaaagtctccgaacgtgtcacgttctcttgaaacgtgacacgttcggagaca-3') targeting sequences cloned into pLentiLox 3.7-Puro was used as a control. Lentiviral transduced ID8-IP cells were selected by growth in puromycin, cell clones were isolated by single cell sorting (FACS Aria, BD Biosciences) into 96 well plates, expanded, and characterized by immunoblotting for FAK. Three cell clones were pooled, expanded, and stored frozen as stable pools of Scr- or FAK shRNA-expressing ID8-IP cells. shRNA-resistant FAK

constructs were created by site-directed mutagenesis using the forward (5'-gaagaaggtatttgctatctgacagacaaaggctgc-3') and reverse (5'-ctgtcagatagcaaataccttcttctgggccgattg-3') primers targeting the coding sequence for FAK residues (279-282) but do not change the translated amino acids in this region. Green fluorescent protein (GFP) tagged FAK-wildtype (WT) or FAK kinase-dead (KD) in pEGFP-C1 [35] were mutated into shRNA-resistant constructs and subcloned into the lentiviral vector pCDH1-MCS1-EF1-Puro (System Biosciences). For reconstitution studies, FAK shRNA ID8-IP cells were lentiviral transduced to express GFP-FAK WT or GFP-FAK KD, sorted by flow cytometry, and used directly in experimental analyses within 10-14 days.

Cell growth assays

Cells were plated under adherent (5×10^4 cells, tissue culture-treated) and non-adherent conditions (2.5×10^5 cells, poly-HEMA-coated) in 6-well plates (Costar) in 2 ml growth media. Between 24 and 144 hours, all cells were collected by limited trypsin-EDTA treatment, a single cell suspension was prepared, and the viable total cell number determined by automated trypan blue staining and counting (ViCell XR, Beckman). For soft agar assays, 48-well plates were coated with a 1:4 dilution of 2% agar (EM Science) in 0.2 ml growth media (bottom layer). For each well, 1×10^4 cells per well were plated in 0.3% agar in 0.2 ml growth media (middle layer). After solidification, a top layer of 0.3% agar in 0.15 ml of growth media was added. Cell growth media (0.2 ml) was added and either DMSO or PF-271 added (inhibitor concentration determined for 0.75 ml total volume). After 7 days, colonies were stained with crystal violet, imaged in phase contrast, and enumerated by counting the center field of each well. All experimental points were performed in triplicate or quadruplicate and repeated two or three times.

Immunoblotting

Protein extracts of cells were made using lysis buffer (RIPA) containing 1% Triton X-100, 1% sodium deoxycholate, 0.1% SDS, 50 mM Hepes pH 7.4, 150 mM NaCl, 10% glycerol, 1.5 mM $MgCl_2$, 1 mM EGTA, 10 mM sodium pyrophosphate, 100 mM NaF, 1 mM sodium orthovanadate, and 10 μg/ml leupeptin. Tumors were resected and homogenized using a Pro 200 tissue homogenizer (Pro Scientific) in RIPA lysis buffer without sodium deoxycholate and SDS. Total protein levels were determined by bicinchoninic acid assay (Pierce), proteins were resolved by NuPAGE 4-12% Tris-Bis gels (Invitrogen), and transferred to polyvinylidene difluoride membranes (Immobilon, Millipore) for antibody immunoblotting. Ratios of pY397 FAK to total FAK and pY416 c-Src to total c-Src analyses were performed by sequential reprobing of membranes as described [36]. Relative expression levels and phospho-specific antibody reactivity were measured by densitometry analyses of blots using Image J (Version 1.43).

Immunohistochemistry

Tumors were divided into thirds and either fixed in formalin, snap-frozen in Optimal Cutting Temperature (OCT) compound (Tissue Tek), or processed for protein lysates (as above). Formalin-fixed tumors were paraffin-embedded, sectioned, and processed for hematoxylin and eosin (H&E) staining. To visualize mCherry tumor-associated protein expression, formalin-fixed paraffin-embedded sections were incubated at 60°C for 30 min, deparaffinized in xylene washes, and rehydrated in ethanol/water washes. Antigen retrieval (boiling for 10 min in 10 mM sodium citrate pH 6) and peroxidase quenching (0.3% hydrogen peroxide for 10 min) were performed. Sections were incubated in Blocking Buffer (PBS with 5% normal goat serum, 0.5% BSA, and 0.1% Triton X-100) for 45 min at room temperature and then incubated with anti-DsRed polyclonal antibody (Clontech 1:100 dilution in Blocking Buffer) overnight. Biotinylated goat-anti-rabbit IgG (1:300), Vectastain ABC elite, and diaminobenzidine (Vector Labs) were used to visualize DsRed antibody

binding and slides were counter-stained with hematoxylin. Images were captured at 4X, 10X, and 20x, using an inverted microscope (Nikon Eclipse Ti 90), color camera (Nikon DS-Fi1), and NIS Elements software (Nikon).

For apoptosis and anti-CD31 staining analyses, frozen tumors were thin sectioned (7 μm) using a cryomicrotome (Leica CM1950) and mounted onto glass slides. Sections were fixed with acetone, permeabilized in PBS/0.5% BSA for 5 min, and blocked with 8% goat serum in PBS/0.5% BSA for 30 min at room temperature. Tumor apoptosis was measured by terminal deoxynucleotidyl transferase dUTP nick end labeling (TUNEL) staining using the fluorescein isothiocyanate (FITC) kit as per the manufacturer's instructions (Roche). For CD31 staining, sections were fixed in acetone, rinsed in 0.5% BSA and PBS, and blocked with a solution of PBS containing 0.5% BSA and 1% goat serum. FITC-conjugated anti-CD31 antibodies at 1 μg/ml in 0.5% BSA and PBS were incubated overnight. Cell nuclei were visualized by incubation with 1:50,000 dilution of Hoechst 33342 (Invitrogen). Images were sequentially captured at 10X and 40X (UPLFL objective, 1.3 NA; Olympus) using a monochrome charge-coupled camera (ORCA ER; Hamamatsu), an inverted microscope (IX81; Olympus), and Slidebook software (v5.0, Intelligent Imaging). Images were pseudo-colored, overlaid, merged using Photoshop CS3 (Adobe), and quantified using Image J (v1.43).

Mice

Female C57BL/6 mice (Charles River) were housed in pathogen-free conditions according Association for the Assessment and Accreditation for Laboratory Animal Care guidelines. Studies were performed with approved institutional animal care and use protocols and adhere to ARRIVE guidelines. No body weight loss or morbidity was associated with the study protocols.

Orthotopic tumor model

Growing tumor cells were harvested by limited trypsinization, washed in PBS, and counted (ViCell XR, Beckman). Surgical implantation of mCherry-labeled ID8 or ID8-IP cells unilaterally under the bursa surrounding the ovary of 8-10 week old C57Bl6 mice was performed as described [37]. Briefly, 0.5×10^6 (non-inhibitor) or 0.75×10^6 (inhibitor) cells were mixed with growth factor-depleted Matrigel (BD Biosciences) injected (7 μl) using a Hamilton syringe, 29.5 gauge needle, and incisions closed with surgical staples. Mice were evaluated daily for signs of distress and initiation of FAK inhibitor or vehicle administration started at Day 7 and was maintained through termination. All mice were euthanized at Day 28, at which time ascites was collected and peritoneal washings performed with 5 mL of PBS, ovary-tumor and uterine horns removed-photographed, and the tumor was dissected and weighed. In peritoneal washings, erythrocytes were lysed using RBC lysis buffer (eBioscience), cells collected by centrifugation, enumerated (ViCell XR), and then fixed in 4% paraformaldehyde. The percent of mCherry-positive tumor cells was determined by flow cytometry (FACSAria, BD Biosciences) and the number of ascites-associated tumor cells was determined by multiplying the total cell number by the percent of mCherry-positive cells. For evaluation of tumor spread, fluorescent images of the intra-abdominal cavity and internal organs (intestines, lungs, spleen, omentum, kidneys, uterus, contralateral ovary, and diaphragm) were acquired using an OV100 Small Animal Imaging System (Olympus). For quantitation, a common threshold for mCherry fluorescence was set and metastatic sites were enumerated using Image J.

Database analyses

The cBio Cancer Genomics Portal was accessed (http://www.cbioportal.org/public-portal/). All cancer studies were queried for percentage of *Ptk2* gene amplification in different

cancers and significance determined by Chi-squared test using Prism (GraphPad Software, v5.0d). Expression array data was evaluated using the online tool termed the Kaplan-Meier Plotter (http://www.kmplot.com/ovar) as described [38]. The datasets include gene expression and survival data from Gene Expression Omnibus and The Cancer Genome Atlas (Affymetrix HG-U133A, HG-U133A 2.0, and HG-U133 Plus 2.0 microarrays). The probe set used for *Ptk2* analyses was 208820_at that contains 11 antisense probes. Query parameters were: overall survival, split patients by median, auto-select best cut-off, and follow up threshold of 10 years. Signal range of the probe was 369-9759 and the auto-cutoff value was 1861. Restriction analyses were stage (all), histology (serous), grade (all), debulk (all), and chemotherapy treatments (all). 961 patient samples were analyzed.

Statistics

Significant difference between groups was determined using one-way ANOVA with Tukey post hoc. Differences between pairs of data were determined using an unpaired two-tailed student's t-test. All statistical analyses were performed using Prism (GraphPad Software, v5.0d). p-values of <0.05 were considered significant.

Results

Elevated FAK expression in ovarian cancer and connections to patient survival

Previous immunohistochemical studies of serous ovarian carcinoma patient samples revealed that FAK overexpression was correlated with advanced tumor stage, elevated tumor grade, tumor-positive lymph nodes, and the presence of distant metastasis [15,16]. In a sample size of ~80 paraffin-embedded sections, FAK over-expression was associated with poor patient survival [16]. Changes in FAK expression can occur through gene amplification events [39] and analyses of The Cancer Genome Atlas (TCGA) database revealed that FAK (*Ptk2*) gene amplification occurred in 24% of serous ovarian patient cohort samples analyzed (Fig. 1A). The rate of *Ptk2* amplification in serous ovarian cancer is significantly higher than breast, prostate, colon, and a variety of other well-characterized cancer patient cohorts documented in the TGCA database (Fig. 1A).

To extend these observations, Kaplan-Meier survival analyses of serous ovarian cancer patient mRNA samples were compared by analysis of a microarray database containing 22,227 genes and annotated patient outcomes (http://www.kmplot.com/ovar) [38]. By comparison of 961 patient samples without restriction for tumor stage, grade, status of tumor debulking or chemotherapy treatments, high FAK mRNA levels were associated with significantly worse overall patient survival (logrank $P = 0.0007$) over ten years (Fig. 1B). Together, this supports the notion that *Ptk2* gene amplification in serous ovarian carcinoma may result in elevated FAK expression and a poor patient prognosis.

Isolation of aggressive murine ovarian carcinoma cells

FAK signaling within tumor cells can alter the tumor microenvironment by regulating the expression of proteases [40], growth factors [41], and cell surface-associated proteins influencing inflammation [12]. In order to study these events, as well as establish a tumor model system that is compatible with conditional FAK knockout or knockin mice on C57Bl6 backgrounds [42,35], we re-isolated murine ID8 ovarian carcinoma cells [34] after intraperitoneal growth in C57Bl6 mice for 43 days (Fig. 2). Ascites-associated cells were cultured in suspension using poly-HEMA plates for 4 weeks, and a pooled population of cells was established (ID8-IP, Fig. 2A). Comparisons of ID8 and ID8-IP in culture showed that ID8-IP cells grew to higher cell densities under adherent conditions (Fig. 2B) and ID8-IP but not ID8 cells could proliferate in suspension culture (Fig. 2C). At high densities, cell morphology was different with ID8 cells establishing a monolayer and ID8-IP cells

exhibiting focus formation (Fig. 2D). Large spheroid formation was not observed with ID8 or ID8-IP cells (Fig. 2D). In soft agar, ID8-IP cells formed significantly more colonies than ID8 after 7 days (Fig. 2E). Together, these results show that ID8-IP cells exhibit traits consistent with a higher degree of cell transformation.

To evaluate potential cell-associated protein changes, immunoblotting was performed on ID8 and ID8-IP cell lysate and revealed E-cadherin down-regulation in ID8-IP cells (Fig. 2F). This is consistent with a potential loosening of cell attachments and ability to shed tumor cells into the peritoneal cavity [43]. E-cadherin expression was maintained in ID8 cells grown on poly-HEMA-coated dishes (Suspended) for 3 days. Under suspended conditions, indirect markers of FAK (Y397 phosphorylation, pY397) or c-Src (Y416 phosphorylation, pY416) activation were low in ID8 cells (Fig. 2F). In contrast, both FAK pY397 and c-Src pY416 phosphorylation were high in adherent ID8-IP cells and FAK-Src activation was maintained in ID8-IP cells grown in suspension for 3 days (Fig. 2F). Thus, increased FAK and c-Src activity were detected in lysates of suspended ID8-IP but not parental ID8 cells.

ID8-IP cells exhibit enhanced tumor growth and metastasis after orthotopic implantation in C57Bl6 mice

Cell implantation within the murine peri-ovarian bursa space provides an optimal microenvironment to monitor serous ovarian carcinoma tumor growth and spread [37]. ID8 and ID8-IP cells were transduced to express the fluorescent mCherry protein and injected into the peri-ovarian bursa space of C57Bl/6 mice (Fig. 3). After 28 days, ID8-IP tumors were larger and exhibited macroscopic fluorescent spread to the tissues surrounding the ovary compared to the smaller ID8 tumors that remained confined within the injected area (Fig. 3A and B). Quantification of tumor progression showed that ID8-IP tumors were larger and shed an increased number of tumor cells into the peritoneal space as collected with ascites and peritoneal washes (Figs. 3C and D). ID8-IP tumors exhibited increased metastatic spread to other organs (colon, stomach, kidney, liver, spleen, and diaphragm, data not shown) and the peritoneal wall after 28 days compared ID8 cells grown as tumors (Fig. 3E). Differences between the growth and spread of ID8 versus ID8-IP ovary-associated tumors were also visualized by H&E and immunohistochemical staining to detect mCherry-expressing tumor cells (Fig. 4A and B). ID8 tumors were detected within the peri-ovarian space or within the bursa-associated mesothelium (Fig. 4A). Larger ID8-IP tumors exhibited infiltration within various surrounding tissues and tumor cell penetration of the ovary (Fig. 4B). Orthotopic ID8-IP tumor growth and spread exhibits many parallels with clinical patterns of human epithelial ovarian carcinoma clinical progression.

Pharmacological inhibition of FAK prevents suspended ID8-IP growth independent of effects on c-Src

The small molecule FAK inhibitor PF-271 exhibits nanomolar IC50 activity against FAK in various tumor cell lines and 100-fold greater concentrations are required for effects against Src-family tyrosine kinases [21]. Treatment of adherent ID8 and ID8-IP cells with PF-271 revealed that concentrations below 1 μM were ineffective in altering cell growth over 6 days (Fig. 5A). However, 0.1 and 0.5 μM PF-271 significantly prevented ID8-IP anchorage-independent growth on poly-HEMA plates (Fig. 5B) and in soft agar (Fig. 5C). Pharmacological FAK inhibition also prevented the proliferation of human ovarian carcinoma cells IGROV1, HEY, and A2780 but not SKOV3 or 2008 cells under suspended culture conditions (Fig. S1). Notably, 0.1 and 0.5 μM PF-271 treatment of ID8-IP cells for 24 h selectively inhibited FAK Y397 phosphorylation without altering Src Y416 phosphorylation under suspended culture conditions (Fig. 5D). These results support the

importance of FAK activity in promoting the anchorage-independent growth of ID8-IP and other human ovarian carcinoma cells.

Oral PF-271 administration prevents ID8-IP tumor growth and metastasis

Studies in human xenograft or syngeneic mouse tumor models have associated PF-271 oral administration with the inhibition of breast, liver, prostate, pancreatic, and squamous cell carcinoma tumor growth [21,26-32]. Dosing has ranged from 5 to 50 mg/kg and twice-daily administration (BID) has shown greatest efficacy [21]. Although other small molecule FAK inhibitors have been tested using IP injection of ovarian carcinoma cells [22,23], true orthotopic models combined with pharmacological inhibition have not been tested for ovarian cancer and the in vivo effect of FAK inhibition in such a model remains unknown.

To determine the effect of FAK inhibition in vivo, mCherry-labeled ID8-IP cells were surgically injected into the ovarian bursa and after 7 days, oral administration of PF-271 at 30 mg/kg or vehicle was initiated every 12 h (Fig. 6). Mice maintained normal weight and habitus. At experimental day 28, mice were euthanized and PF-271 treated mice showed significantly smaller primary tumors and less peritoneal metastasis than vehicle-treated control mice (Figs. 6A and B). Inhibition of orthotopic ID8-IP tumor growth was also obtained after twice-daily administration of a different FAK inhibitor (PND-1186 at 150 mg/kg) compared to vehicle-treated mice (Fig. S2).

Analyses of primary tumors by immunoblotting showed that FAK phosphorylation at Y397 was high in vehicle-treated controls, normalized to the level of FAK expression and Y397 FAK phosphorylation in normal mouse ovary samples (Figs. 6C and D). Densitometry of immunoblots showed that PF-271 treatment significantly inhibited FAK Y397 phosphorylation compared to vehicle-treated tumors (Figs. 6C and D). Inhibition of FAK Y397 phosphorylation also occurred after PND-1186 treatment of tumors (Fig. S2). Interestingly, c-Src expression levels were elevated in ovary-associated ID8-IP tumors compared to normal ovary tissue, normalized to actin levels (Fig. 6C). However, PF-271 treatment did not reduce c-Src Y416 phosphorylation in ID8-IP tumors (Fig. 6E). Together, these results show that PF-271 inhibition of FAK blocks ID8-IP tumor growth and spread through a mechanism that is independent of inhibitory effects on Src Y416 phosphorylation either in vitro (Fig. 5) or in vivo (Fig. 6).

To elucidate a potential mechanism associated with PF-271 inhibition of ID8-IP, primary tumor growth, tumor sections were analyzed by staining (Fig. 7). H&E staining revealed a high density of tumor cells within ovaries of vehicle-treated mice (Fig. 7A). Ovaries of PF-271-treated mice contained tumor cells, but cell density was lower (Fig. 7A) and the recovered tumors were of fragile or friable state. Frozen section analyses of tumors revealed fewer CD31-positive endothelial cells (Figs. 7B and C) and increased levels of cell apoptosis as determined by TUNEL staining (Figs. 7D and E) in PF-271-treated tumors compared to vehicle-treated controls. Thus, decreased tumor-associated endothelial cell density and increased tumor cell apoptosis are potential mechanisms associated with PF-271 inhibition of ID8-IP tumor growth.

Confirmation of the importance of FAK kinase activity in promoting anchorage-independent ID8-IP cell survival

Pharmacological FAK inhibition can alter both tumor cell intrinsic and tumor micro-environmental properties. To determine if PF-271-mediated inhibition of ID8-IP cell growth under suspended cell conditions is due to the loss of FAK activity, FAK knockdown and re-expression analyses were performed (Fig. 8). Pooled populations of cells stably expressing lentiviral scrambled (Scr) or anti-FAK shRNA were selected by growth in puromycin. Cells

were transduced with shRNA-resistant green fluorescent protein (GFP) tagged FAK wildtype (WT) or GFP-FAK kinase dead (KD), sorted by flow cytometry, expanded, and used for proliferation-survival experiments within 10-14 days. GFP-FAK WT or GFP-FAK KD levels were verified by flow cytometry (Fig. 8A) and by immunoblotting (Fig. 8B) prior to experiments. Scr and FAK shRNA-expressing ID8-IP cells were transduced with GFP and expression levels verified by flow cytometry (Fig. S3). The same number of Scr shRNA, FAK shRNA, FAK shRNA + GFP-FAK WT, or FAK shRNA + GFP-FAK KD were evaluated for growth under adherent (Fig. 8C) or suspended conditions (Fig. 8D) over 5 days.

Reduction in FAK expression or re-expression of FAK-KD did not alter ID8-IP cell viability under adherent conditions. However, FAK knockdown slightly reduced adherent cell growth and this was rescued by either FAK-WT or FAK-KD re-expression (Fig. 8C). Under suspended conditions, FAK knockdown reduced cell viability and this remained constant with FAK-WT or FAK-KD re-expression (Fig. 8D). Strikingly, major differences in ID8-IP cell numbers after 5 days were observed upon FAK knockdown compared to Scr shRNA ID8-IP control cells that continued to proliferate (Fig. 8D). Notably, FAK-WT re-expression promoted survival and growth of FAK shRNA-expressing ID8-IP under suspended conditions (Fig. 8D). In contrast, the percent of initial FAK-KD expressing cells was reduced after 5 days. These genetic results confirm and extend pharmacological findings that FAK activity is required for anchorage-independent ID8-IP cell proliferation. Together, these results support the conclusion that cell intrinsic and FAK-associated signals promote the aggressive phenotype of ID8-IP tumors in mice.

Discussion

This is the first study to utilize an orthotopic syngeneic murine model to evaluate the role of FAK activity in ovarian cancer tumor progression. The injection of cells within the bursal peri-ovarian space provides an advantage over intraperitoneal injection since bursal injection allows for the measureable growth of a primary tumor within the ovarian microenvironment that can spread to distant sites within the peritoneum. This model replicates ovarian cancer clinical progression in humans as patients can present with a primary ovarian tumor associated with local invasion and intra-abdominal metastases [44]. As diffuse colonization of the peritoneum is usually seen in later stages, it is believed that the ovarian tumor arises first and then sheds cells which seed other sites.

For analysis of rapid orthotopic tumor growth, we generated a new murine ovarian cancer cell line, named ID8-IP, which was recovered from ascites of mice injected intraperitoneally with ID8 cells. Previous studies have isolated aggressive ID8 cells after orthotopic injection exhibiting an increased rate of lethal tumor progression reduced to 60 days compared to 114 days for parental ID8 cells [44]. ID8-IP cells exhibit an accelerated rate of tumor progression with lethality occurring within 40 days. We speculate that the growth of ID8-IP cells initially as spheroids within the peritoneal cavity and then selected for anchorage-independent growth in culture, may have contributed to the aggressive ID8-IP phenotype. Both FAK and Src tyrosine kinase activity are elevated within ID8-IP cells cultured in suspension. Notably, the subcutaneous passage of lymphoma cells in mice also resulted in increased FAK expression within recovered tumor cells [45]. The importance of FAK signaling facilitating the establishment, growth, or survival of tumor cells in mice is supported by studies using conditional FAK knockout mice [46-48,29].

Analyses of the TCGA database revealed that FAK gene amplification occurs significantly more often in serous human ovarian cancer compared to other cancers such as those of breast, prostate, and colon; which also tend not to spread exfoliatively and/or form ascites.

Moreover, Kaplan-Meier analyses of 961 patient samples revealed that high FAK mRNA levels were associated with significantly worse overall patient survival (logrank $P = 0.0007$) over ten years. Importantly, ID8-IP cells were sensitive to low nanomolar concentrations of PF-271 in the selective prevention anchorage-independent growth. Oral administration of PF-271 inhibited ID8-IP orthotopic tumor growth and prevented peritoneal metastasis. Much of the literature concerning FAK is based upon studies of cells grown adherently in 2D (two-dimensional) culture on plastic dishes and it remains undetermined how FAK promotes ovarian carcinoma tumor growth in suspension. However, this sensitivity to the inhibition of FAK expression or activity only under conditions of anchorage-independence was also observed with breast carcinoma cells using the PND-1186 small molecule FAK inhibitor [23]. Tumor growth using spheroids may better reflect *in vivo* tumor biology, particularly in ovarian cancer, where spheroids are thought to represent a common mechanism of dissemination. Ongoing studies are testing the hypothesis that FAK activity may facilitate integrin interactions with adhesion molecules on neighboring tumor cells, and thus promote cell survival signaling within the spheroid. Thus, therapeutic anti-integrin [49] and FAK inhibitors may target critical signaling pathways within a spheroid environment needed for ovarian cancer survival as well as in established tumors and metastases.

Notably, PF-271 addition to ID8-IP cells did not prevent activation-associated Src tyrosine phosphorylation at Y416 in suspended cells or in tumors under conditions where FAK Y397 phosphorylation was inhibited and tumor growth prevented. Although recent studies using squamous carcinoma cells suggest that FAK inhibition triggers autophagic targeting of Src to promote cancer cell survival [50], PF-271 treatment of these cells results in combined FAK and Src inhibition [32]. It is unclear whether this is unique to squamous carcinoma cells as PND-1186 FAK inhibitor treatment of 4T1 breast carcinoma cells resulted in FAK but not Src inhibition in cell culture and tumors [23,24]. Further studies are needed to determine if pharmacological FAK inhibition alters ovarian carcinoma cell signaling pathways independently of effects on Src.

Our orthotopic tumor studies also revealed that PF-271 reduced the number of endothelial cells within tumors and this was associated with increased levels of tumor apoptosis. Similar findings were observed in the first PF-271 study of H125 lung tumor cell xenografts [21] and this has been extended to pharmacological FAK inhibition in ovarian [22] and colon [51] cancer xenografts. PF-271 blocks blood vessel sprouting in chicken chorioallantoic membrane assays [52] and mouse aortic explant assays [42]. A related Pfizer compound (PF-573,228) reduces human umbilical cord vein endothelial cell viability, migration, and tube formation in vitro [53]. The strongest support for the importance of FAK activity in promoting vascular remodeling comes from the generation of kinase-inactive FAK knockin mice whereby embryonic lethality was associated with the lack of yolk sac capillary plexus formation and disorganized endothelial cell patterning [35,54]. With the creation of an inducible FAK kinase-inactive knockin within adult mouse endothelial cells [55], and the back-crossing of this mouse onto a pure C57Bl/6 background, future experiments with ID8-IP cells should be able to selectively evaluate the contribution of FAK activity within endothelial cells in promoting ovarian tumor progression.

Besides acting on ovarian tumor cells and endothelial cells, PF-271 treatment can also interfere with tumor-associated fibroblast and macrophage recruitment [31]. Moreover, PND-1186 FAK inhibitor administration was shown to decrease leukocyte infiltrate and reduce breast tumor-associated splenomegaly [24]. As low level stimulation of inflammatory mediators such as tumor necrosis factor-α (TNF-α) can contribute to the pathogenesis of ovarian cancer [56], and FAK activity controls gene expression events in response to TNF-α within endothelial cells [57,12], it is possible that the PF-271 inhibition of FAK activity

within various stromal-associated cells may also alter the course of ovarian tumor progression.

Overall, primary chemotherapy is very effective in initial ovarian cancer treatment. However, the majority of patients will succumb to chemoresistant reoccurrence and metastasis. Thus, combinations of FAK inhibitors with other chemotherapy regimens may further improve efficacy and prevent recurrences [22,31]. For example, combinations of PF-271 with another tyrosine kinase inhibitor (sunitinib) had enhanced anti-tumor effects [28]. Clearly, further studies are needed to elucidate the key cell targets and FAK-associated signaling pathways promoting ovarian tumor progression in order to optimize combinations of chemotherapeutics.

In summary, we show that FAK activity is important for growth and metastasis of ovarian cancer, both in vitro and in vivo. Targeting FAK activity with pharmacological inhibitors in human ovarian cancer could be an important step in decreasing the mortality from this disease. As small molecule FAK inhibitors have been found to be safe and well tolerated in animal studies, and Phase I human studies of PF-271 of highly treated patient populations are encouraging as 12% of patients showed stable disease [25], our studies support potential Phase II clinical trials with small molecule FAK inhibitors in ovarian cancer.

Supplementary Material

Refer to Web version on PubMed Central for supplementary material.

Acknowledgments

We appreciate the generosity of Joan Wyllie and “Nine Girls Ask?” for the purchase of a ViCell XR cell viability analyzer and a Leica CM1950 cryostat used in this study. PND-1186 was obtained from Poniard Pharmaceuticals. This work was supported by National Institutes of Health grants (CA102310 and GM087400) to D.D. Schlaepfer. K. Ward is a fellow of the UCSD Reproductive Medicine Gynecological Oncology program. I. Tancioni was supported by a grant from Susan G. Komen for the Cure (KG111237), C. Lawson was supported by a Canadian Institutes of Health Research fellowship (200810MFE-193594-139144), N.L.G. Miller was supported by a National Research Service Award (1F32CA159558), C. Jean was supported by an American Heart Association fellowship (12POST11760014), and D. Stupack was supported by National Institutes of Health grant (CA107263).

Abbreviations

ANOVA	analysis of variance
BSA	bovine serum albumin
DMSO	dimethylsulfoxide
EDTA	Ethylenediaminetetraacetic acid
FACS	fluorescence-activated cell sorting
FAK	focal adhesion kinase
FBS	fetal bovine serum
FITC	fluorescein isothiocyanate
GFP	green fluorescent protein
IP	intraperitoneal
KD	kinase dead
OCT	Optimal Cutting Temperature

PBS	phosphate-buffered saline
PF-271	PF-562,271
PFA	paraformaldehyde
Poly-HEMA	polyhydroxyethylmethacrylate
shRNA	Short hairpin RNA
TUNEL	terminal deoxynucleotidyl transferase dUTP nick end labeling
WT	wild type

References

1. Siegel R, Naishadham D, Jemal A. Cancer statistics, 2012. CA Cancer J Clin. 2012; 62:10–29. [PubMed: 22237781]
2. Agarwal R, Kaye SB. Ovarian cancer: strategies for overcoming resistance to chemotherapy. Nat Rev Cancer. 2003; 3:502–516. [PubMed: 12835670]
3. Bast RC Jr. Hennessy B, Mills GB. The biology of ovarian cancer: new opportunities for translation. Nature Rev Cancer. 2009; 9:415–428. [PubMed: 19461667]
4. Cannistra SA. Cancer of the ovary. N Engl J Med. 2004; 351:2519–2529. [PubMed: 15590954]
5. Landen CN Jr. Birrer MJ, Sood AK. Early events in the pathogenesis of epithelial ovarian cancer. J Clin Oncol. 2008; 26:995–1005. [PubMed: 18195328]
6. Shield K, Ackland ML, Ahmed N, Rice GE. Multicellular spheroids in ovarian cancer metastases: Biology and pathology. Gynecol Oncol. 2009; 113:143–148. [PubMed: 19135710]
7. Lengyel E. Ovarian cancer development and metastasis. Am J Pathol. 2010; 177:1053–1064. [PubMed: 20651229]
8. Berns EM, Bowtell DD. The changing view of high-grade serous ovarian cancer. Cancer Res. 2012; 72:2701–2704. [PubMed: 22593197]
9. Zhao J, Guan JL. Signal transduction by focal adhesion kinase in cancer. Cancer Met Rev. 2009; 28:35–49.
10. Schaller MD. Cellular functions of FAK kinases: insight into molecular mechanisms and novel functions. J Cell Sci. 2010; 123:1007–1013. [PubMed: 20332118]
11. Lim ST, Chen XL, Lim Y, Hanson DA, Vo TT, Howerton K, Larocque N, Fisher SJ, Schlaepfer DD, Ilic D. Nuclear FAK promotes cell proliferation and survival through FERM-enhanced p53 degradation. Mol Cell. 2008; 29:9–22. [PubMed: 18206965]
12. Lim ST, Miller NL, Chen XL, Tancioni I, Walsh CT, Lawson C, Uryu S, Weis SM, Cheresh DA, Schlaepfer DD. Nuclear-localized focal adhesion kinase regulates inflammatory VCAM-1 expression. J Cell Biol. 2012; 197:907–919. [PubMed: 22734001]
13. Goode EL, Chenevix-Trench G, Song H, Ramus SJ, Notaridou M, Lawrenson K, Widschwendter M, Vierkant RA, Larson MC, Kjaer SK, Birrer MJ, Berchuck A, Schildkraut J, Tomlinson I, Kiemeney LA, Cook LS, Gronwald J, Garcia-Closas M, Gore ME, Campbell I, Whittemore AS, Sutphen R, Phelan C, Anton-Culver H, Pearce CL, Lambrechts D, Rossing MA, Chang-Claude J, Moysich KB, Goodman MT, Dork T, Nevanlinna H, Ness RB, Rafnar T, Hogdall C, Hogdall E, Fridley BL, Cunningham JM, Sieh W, McGuire V, Godwin AK, Cramer DW, Hernandez D, Levine D, Lu K, Iversen ES, Palmieri RT, Houlston R, van Altena AM, Aben KK, Massuger LF, Brooks-Wilson A, Kelemen LE, Le ND, Jakubowska A, Lubinski J, Medrek K, Stafford A, Easton DF, Tyrer J, Bolton KL, Harrington P, Eccles D, Chen A, Molina AN, Davila BN, Arango H, Tsai YY, Chen Z, Risch HA, McLaughlin J, Narod SA, Ziogas A, Brewster W, Gentry-Maharaj A, Menon U, Wu AH, Stram DO, Pike MC, Beesley J, Webb PM, Chen X, Ekici AB, Thiel FC, Beckmann MW, Yang H, Wentzensen N, Lissowska J, Fasching PA, Despierre E, Amant F, Vergote I, Doherty J, Hein R, Wang-Gohrke S, Lurie G, Carney ME, Thompson PJ, Runnebaum I, Hillemanns P, Durst M, Antonenkova N, Bogdanova N, Leminen A, Butzow R, Heikkinen T, Stefansson K, Sulem P, Besenbacher S, Sellers TA, Gayther SA, Pharoah PD. A genome-wide

association study identifies susceptibility loci for ovarian cancer at 2q31 and 8q24. Nat Genet. 2010; 42:874–879. [PubMed: 20852632]

14. Network TCGAR. Integrated genomic analyses of ovarian carcinoma. Nature. 2011; 474:609–615. [PubMed: 21720365]
15. Judson PL, He X, Cance WG, Van L. Overexpression of focal adhesion kinase, a protein tyrosine kinase, in ovarian carcinoma. Cancer. 1999; 86:1551–1556. [PubMed: 10526262]
16. Sood AK, Coffin JE, Schneider GB, Fletcher MS, DeYoung BR, Gruman LM, Gershenson DM, Schaller MD, Hendrix MJ. Biological significance of focal adhesion kinase in ovarian cancer: role in migration and invasion. Am J Pathol. 2004; 165:1087–1095. [PubMed: 15466376]
17. Halder J, Landen CN Jr. Lutgendorf SK, Li Y, Jennings NB, Fan D, Nelkin GM, Schmandt R, Schaller MD, Sood AK. Focal adhesion kinase silencing augments docetaxel-mediated apoptosis in ovarian cancer cells. Clin Cancer Res. 2005; 11:8829–8836. [PubMed: 16361572]
18. Halder J, Kamat AA, Landen CN Jr. Han LY, Lutgendorf SK, Lin YG, Merritt WM, Jennings NB, Chavez-Reyes A, Coleman RL, Gershenson DM, Schmandt R, Cole SW, Lopez-Berestein G, Sood AK. Focal adhesion kinase targeting using in vivo short interfering RNA delivery in neutral liposomes for ovarian carcinoma therapy. Clin Cancer Res. 2006; 12:4916–4924. [PubMed: 16914580]
19. Sood AK, Armaiz-Pena GN, Halder J, Nick AM, Stone RL, Hu W, Carroll AR, Spannuth WA, Deavers MT, Allen JK, Han LY, Kamat AA, Shahzad MM, McIntyre BW, Diaz-Montero CM, Jennings NB, Lin YG, Merritt WM, DeGeest K, Vivas-Mejia PE, Lopez-Berestein G, Schaller MD, Cole SW, Lutgendorf SK. Adrenergic modulation of focal adhesion kinase protects human ovarian cancer cells from anoikis. J Clin Invest. 2010; 120:1515–1523. [PubMed: 20389021]
20. Schilder RJ, Brady WE, Lankes HA, Fiorica JV, Shahin MS, Zhou XC, Mannel RS, Pathak HB, Hu W, Alpaugh RK, Sood AK, Godwin AK. Phase II evaluation of dasatinib in the treatment of recurrent or persistent epithelial ovarian or primary peritoneal carcinoma: A Gynecologic Oncology Group study. Gynecol Oncol. 2012 in press.
21. Roberts WG, Ung E, Whalen P, Cooper B, Hulford C, Autry C, Richter D, Emerson E, Lin J, Kath J, Coleman K, Yao L, Martinez-Alsina L, Lorenzen M, Berliner M, Luzzio M, Patel N, Schmitt E, LaGreca S, Jani J, Wessel M, Marr E, Griffor M, Vajdos F. Antitumor activity and pharmacology of a selective focal adhesion kinase inhibitor, PF-562,271. Cancer Res. 2008; 68:1935–1944. [PubMed: 18339875]
22. Halder J, Lin YG, Merritt WM, Spannuth WA, Nick AM, Honda T, Kamat AA, Han LY, Kim TJ, Lu C, Tari AM, Bornmann W, Fernandez A, Lopez-Berestein G, Sood AK. Therapeutic efficacy of a novel focal adhesion kinase inhibitor TAE226 in ovarian carcinoma. Cancer Res. 2007; 67:10976–10983. [PubMed: 18006843]
23. Tanjoni I, Walsh C, Uryu S, Nam JO, Mielgo A, Tomar A, Lim ST, Liang C, Koenig M, Sun C, Kwok C, Patel N, McMahon G, Stupack DG, Schlaepfer DD. PND-1186 FAK inhibitor selectively promotes tumor cell apoptosis in three-dimensional environments. Cancer Biol Ther. 2010; 9:764–777. [PubMed: 20234191]
24. Walsh C, Tanjoni I, Uryu S, Nam JO, Mielgo A, Tomar A, Luo H, Phillips A, Kwok C, Patel N, McMahon G, Stupack DG, Schlaepfer DD. Oral delivery of PND-1186 FAK inhibitor decreases tumor growth and spontaneous breast to lung metastasis in pre-clinical tumor models. Cancer Biol Ther. 2010; 9:778–790. [PubMed: 20234193]
25. Infante JR, Camidge DR, Mileshkin LR, Chen EX, Hicks RJ, Rischin D, Fingert H, Pierce KJ, Xu H, Roberts WG, Shreeve SM, Burris HA, Siu LL. Safety, pharmacokinetic, and pharmacodynamic phase I dose-escalation trial of PF-00562271, an inhibitor of focal adhesion kinase, in advanced solid tumors. J Clin Oncol. 2012; 30:1527–1533. [PubMed: 22454420]
26. Bagi CM, Roberts GW, Andresen CJ. Dual focal adhesion kinase/Pyk2 inhibitor has positive effects on bone tumors: implications for bone metastases. Cancer. 2008; 112:2313–2321. [PubMed: 18348298]
27. Wendt MK, Schiemann WP. Therapeutic targeting of the focal adhesion complex prevents oncogenic TGF-beta signaling and metastasis. Breast Cancer Res. 2009; 11:R68. [PubMed: 19740433]
28. Bagi CM, Christensen J, Cohen DP, Roberts WG, Wilkie D, Swanson T, Tuthill T, Andresen CJ. Sunitinib and PF-562,271 (FAK/Pyk2 inhibitor) effectively block growth and recovery of human

hepatocellular carcinoma in a rat xenograft model. Cancer Biol Ther. 2009; 8:856–865. [PubMed: 19458500]

29. Slack-Davis JK, Hershey ED, Theodorescu D, Frierson HF, Parsons JT. Differential requirement for focal adhesion kinase signaling in cancer progression in the transgenic adenocarcinoma of mouse prostate model. Mol Cancer Ther. 2009; 8:2470–2477. [PubMed: 19671741]
30. Sun H, Pisle S, Gardner ER, Figg WD. Bioluminescent imaging study: FAK inhibitor, PF-562,271, preclinical study in PC3M-luc-C6 local implant and metastasis xenograft models. Cancer Biol Ther. 2010; 10:38–43. [PubMed: 20495381]
31. Stokes JB, Adair SJ, Slack-Davis JK, Walters DM, Tilghman RW, Hershey ED, Lowrey B, Thomas KS, Bouton AH, Hwang RF, Stelow EB, Parsons JT, Bauer TW. Inhibition of focal adhesion kinase by PF-562,271 inhibits the growth and metastasis of pancreatic cancer concomitant with altering the tumor microenvironment. Mol Cancer Ther. 2011; 10:2135–2145. [PubMed: 21903606]
32. Serrels A, McLeod K, Canel M, Kinnaird A, Graham K, Frame MC, Brunton VG. The role of focal adhesion kinase catalytic activity on the proliferation and migration of squamous cell carcinoma cells. Int J Cancer. 2012; 131:287–297. [PubMed: 21823119]
33. Schultze A, Fiedler W. Therapeutic potential and limitations of new FAK inhibitors in the treatment of cancer. Exp Opin Invest Drugs. 2010; 19:777–788.
34. Roby KF, Taylor CC, Sweetwood JP, Cheng Y, Pace JL, Tawfik O, Persons DL, Smith PG, Terranova PF. Development of a syngeneic mouse model for events related to ovarian cancer. Carcinogenesis. 2000; 21:585–591. [PubMed: 10753190]
35. Lim ST, Chen XL, Tomar A, Miller NL, Yoo J, Schlaepfer DD. Knock-in mutation reveals an essential role for focal adhesion kinase activity in blood vessel morphogenesis and cell motility-polarity but not cell proliferation. J Biol Chem. 2010; 285:21526–21536. [PubMed: 20442405]
36. Bernard-Trifilo JA, Lim ST, Hou S, Schlaepfer DD, Ilic D. Analyzing FAK and Pyk2 in early integrin signaling events. Current protocols in cell biology / editorial board, Juan S Bonifacino [et al]. 2006; 14 Unit 14.17.
37. Connolly DC, Hensley HH. Xenograft and Transgenic Mouse Models of Epithelial Ovarian Cancer and Non Invasive Imaging Modalities to Monitor Ovarian Tumor Growth In situ -Applications in Evaluating Novel Therapeutic Agents. Curr Protoc Pharmacol. 2009; 45:1–14.
38. Gyorffy B, Lanczky A, Szallasi Z. Implementing an online tool for genome-wide validation of survival-associated biomarkers in ovarian-cancer using microarray data from 1287 patients. Endocrine-related cancer. 2012; 19:197–208. [PubMed: 22277193]
39. Agochiya M, Brunton VG, Owens DW, Parkinson EK, Paraskeva C, Keith WN, Frame MC. Increased dosage and amplification of the focal adhesion kinase gene in human cancer cells. Oncogene. 1999; 18:5646–5653. [PubMed: 10523844]
40. Mitra SK, Lim ST, Chi A, Schlaepfer DD. Intrinsic focal adhesion kinase activity controls orthotopic breast carcinoma metastasis via the regulation of urokinase plasminogen activator expression in a syngeneic tumor model. Oncogene. 2006; 25:4429–4440. [PubMed: 16547501]
41. Mitra SK, Mikolon D, Molina JE, Hsia DA, Hanson DA, Chi A, Lim ST, Bernard-Trifilo JA, Ilic D, Stupack DG, Cheresh DA, Schlaepfer DD. Intrinsic FAK activity and Y925 phosphorylation facilitate an angiogenic switch in tumors. Oncogene. 2006; 25:5969–5984. [PubMed: 16682956]
42. Weis SM, Lim ST, Lutu-Fuga KM, Barnes LA, Chen XL, Göthert JR, Shen TL, Guan JL, Schlaepfer DD, Cheresh DA. Compensatory role for Pyk2 during angiogenesis in adult mice lacking endothelial cell FAK. J Cell Biol. 2008; 181:43–50. [PubMed: 18391070]
43. Thiery JP, Acloque H, Huang RY, Nieto MA. Epithelial-mesenchymal transitions in development and disease. Cell. 2009; 139:871–890. [PubMed: 19945376]
44. Greenaway J, Moorehead R, Shaw P, Petrik J. Epithelial-stromal interaction increases cell proliferation, survival and tumorigenicity in a mouse model of human epithelial ovarian cancer. Gynecol Oncol. 2008; 108:385–394. [PubMed: 18036641]
45. Bosch R, Moreno MJ, Dieguez-Gonzalez R, Cespedes MV, Gallardo A, Nomdedeu J, Pavon MA, Espinosa I, Mangues MA, Sierra J, Casanova I, Mangues R. Subcutaneous passage increases cell aggressiveness in a xenograft model of diffuse large B cell lymphoma. Clin Exp Metastasis. 2012; 29:339–347. [PubMed: 22262061]

46. McLean GW, Komiyama NH, Serrels B, Asano H, Reynolds L, Conti F, Hodivala-Dilke K, Metzger D, Chambon P, Grant SG, Frame MC. Specific deletion of focal adhesion kinase suppresses tumor formation and blocks malignant progression. Genes Dev. 2004; 18:2998–3003. [PubMed: 15601818]
47. Pylayeva Y, Gillen KM, Gerald W, Beggs HE, Reichardt LF, Giancotti FG. Ras- and PI3K-dependent breast tumorigenesis in mice and humans requires focal adhesion kinase signaling. J Clin Invest. 2009; 119:252–266. [PubMed: 19147981]
48. Luo M, Fan H, Nagy T, Wei H, Wang C, Liu S, Wicha MS, Guan JL. Mammary epithelial-specific ablation of the focal adhesion kinase suppresses mammary tumorigenesis by affecting mammary cancer stem/progenitor cells. Cancer Res. 2009; 69:466–474. [PubMed: 19147559]
49. Sawada K, Ohyagi-Hara C, Kimura T, Morishige K. Integrin inhibitors as a therapeutic agent for ovarian cancer. Journal of oncology. 2012; 2012:915140. [PubMed: 22235205]
50. Sandilands E, Serrels B, McEwan DG, Morton JP, Macagno JP, McLeod K, Stevens C, Brunton VG, Langdon WY, Vidal M, Sansom OJ, Dikic I, Wilkinson S, Frame MC. Autophagic targeting of Src promotes cancer cell survival following reduced FAK signalling. Nat Cell Biol. 2012; 14:51–60. [PubMed: 22138575]
51. Schultze A, Decker S, Otten J, Horst AK, Vohwinkel G, Schuch G, Bokemeyer C, Loges S, Fiedler W. TAE226-mediated inhibition of focal adhesion kinase interferes with tumor angiogenesis and vasculogenesis. Invest New Drugs. 2010; 28:825–833. [PubMed: 19784551]
52. Lim S-T, Mikolon D, Stupack DG, Schlaepfer DD. FERM control of FAK function: Implications for cancer therapy. Cell Cycle. 2008; 7:2306–2314. [PubMed: 18677107]
53. Cabrita MA, Jones LM, Quizi JL, Sabourin LA, McKay BC, Addison CL. Focal adhesion kinase inhibitors are potent anti-angiogenic agents. Mol Oncol. 2011; 5:517–526. [PubMed: 22075057]
54. Zhao X, Peng X, Sun S, Park AY, Guan JL. Role of kinase-independent and -dependent functions of FAK in endothelial cell survival and barrier function during embryonic development. J Cell Biol. 2010; 189:955–965. [PubMed: 20530207]
55. Chen XL, Nam JO, Jean C, Lawson C, Walsh CT, Goka E, Lim ST, Tomar A, Tancioni I, Uryu S, Guan JL, Acevedo LM, Weis SM, Cheresh DA, Schlaepfer DD. VEGF-induced vascular permeability is mediated by FAK. Dev Cell. 2012; 22:146–157. [PubMed: 22264731]
56. Maccio A, Madeddu C. Inflammation and ovarian cancer. Cytokine. 2012; 58:133–147. [PubMed: 22349527]
57. Schlaepfer DD, Hou S, Lim ST, Tomar A, Yu H, Lim Y, Hanson DA, Uryu SA, Molina J, Mitra SK. Tumor necrosis factor-alpha stimulates focal adhesion kinase activity required for mitogen-activated kinase-associated interleukin 6 expression. J Biol Chem. 2007; 282:17450–17459. [PubMed: 17438336]

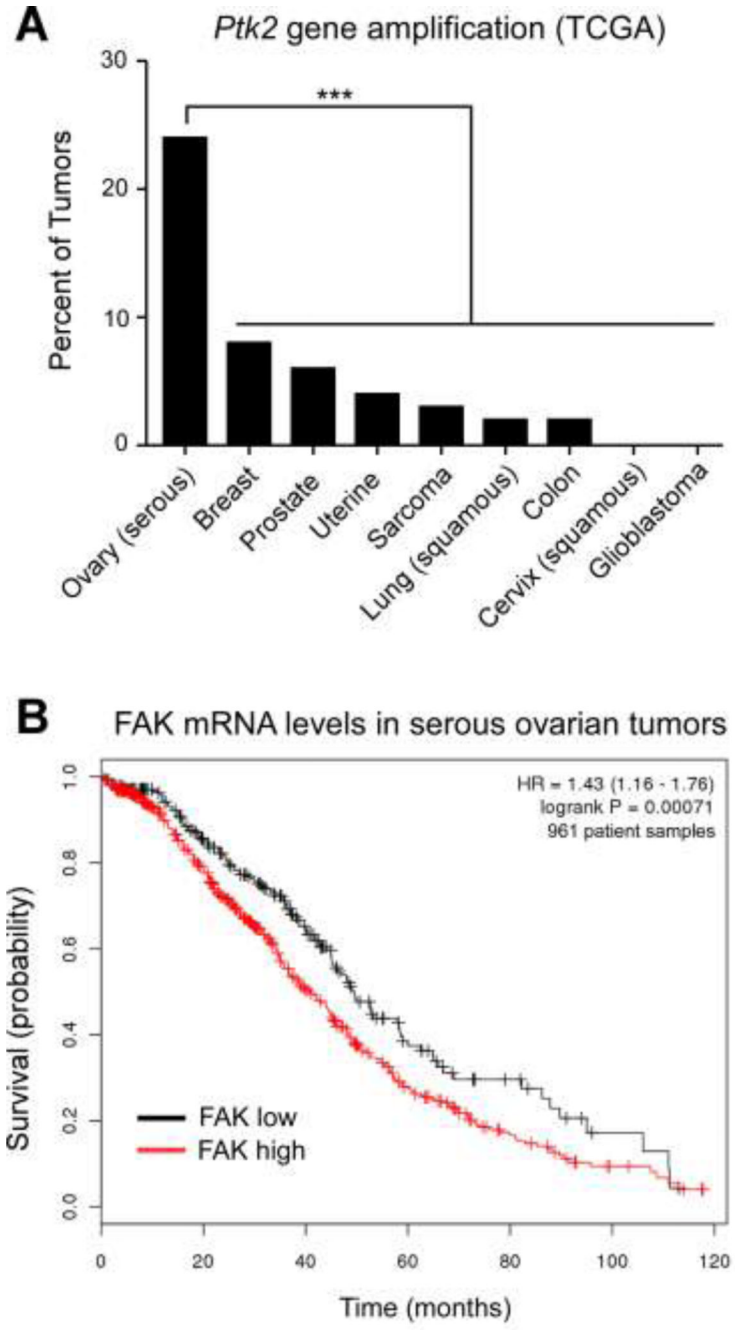

Figure 1.

Elevated FAK gene (*Ptk2*) amplification in ovarian cancer and Kaplan-Meier analyses of FAK mRNA levels with overall patient survival. (A) The cBio Cancer Genomics Portal (http://www.cbioportal.org/public-portal/) was queried for percentage of *Ptk2* gene amplification in The Cancer Genome Atlas (TCGA) with different cancers and significance determined by the Chi-squared test (*** $p<0.001$). (B) The Kaplan-Meier Plotter (http://www.kmplot.com/ovar) was queried to evaluate Affymetrix microarray expression of FAK mRNA levels in 961 annotated serous ovarian cancer patient tumor samples. Selections were: overall survival (follow up threshold of 10 years), split patients by median, stage (all), histology (serous), grade (all), debulk (all), and chemotherapy treatments (all). High levels

of FAK expression (red) are associated with decreased patient survival (logrank $P = 0.0007$) and the Hazard ratio (with 95% confidence intervals) is shown.

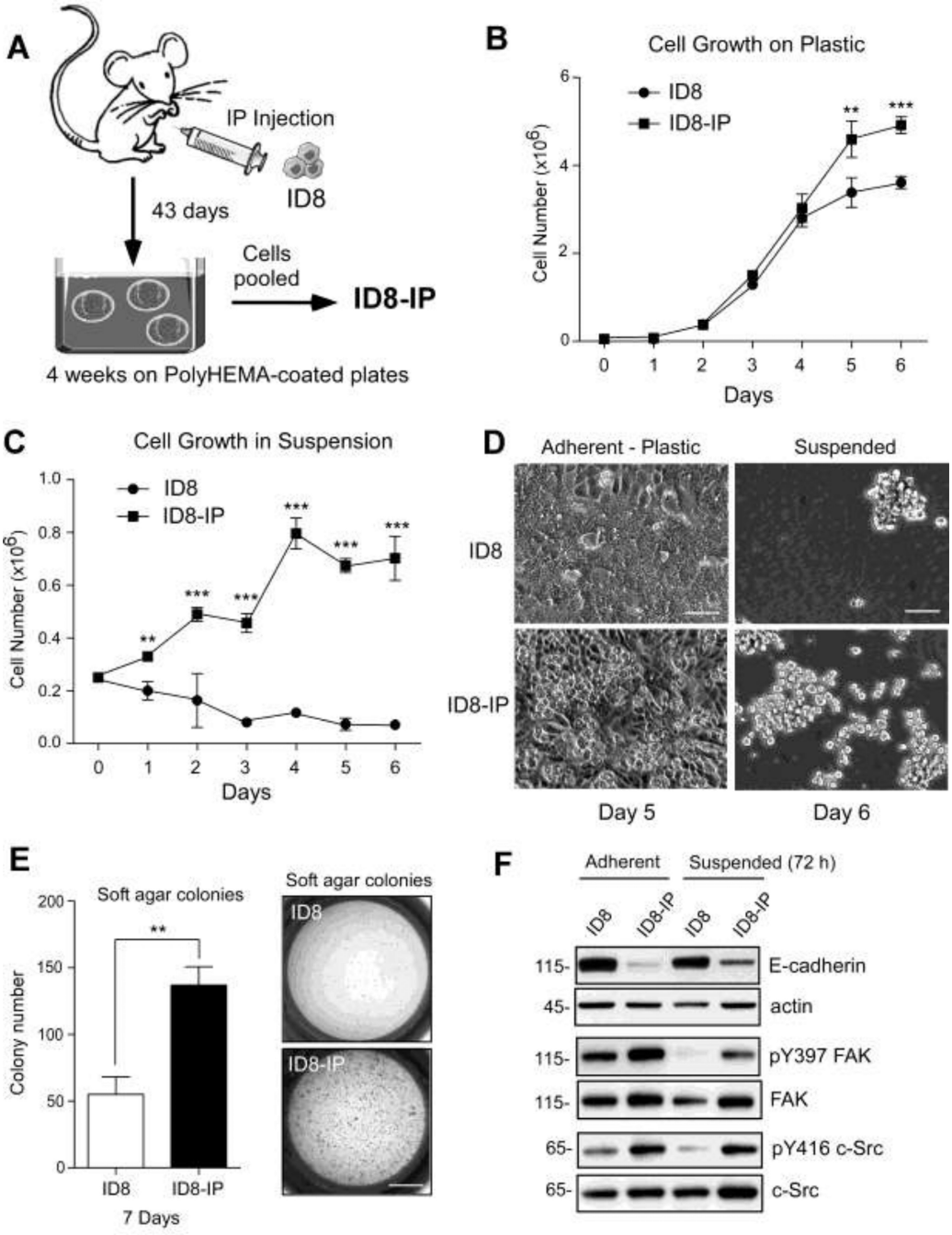

Figure 2.

In vivo passage of ID8 murine ovarian carcinoma cells in C57Bl6 mice result in the spontaneous generation of aggressive cells. (A) Schematic summarizing the intraperitoneal (IP) injection of ID8 cells, re-isolation from ascites after 43 days, growth and expansion in anchorage-independent (poly-HEMA-coated plates) for 4 weeks with the resulting pooled population of cells termed ID8-IP. (B) Adherent proliferation of 50,000 ID8 or ID8-IP cells over 6 days. (C) Anchorage-independent growth of 250,000 ID8 or ID8-IP cells on poly-HEMA coated plates over 6 days. (B and C) Values are means (+/- SD) of triplicate points, (** $p<0.01$, *** $p<0.001$). (D) Phase contrast images of ID8 or ID8-IP cells under adherent and confluent (Day 5) or suspended conditions (Day 6). Scale is 70 μM. (E) Soft agar

colony number of ID8 or ID8-IP cells after 7 days. Values are means (+/- SD) of triplicate points, (** $p<0.01$). Scale is 3 mm. (F) Cell lysates were prepared from ID8 and ID8-IP cells growing under adherent or suspended conditions after 3 days. Total protein was normalized for actin and E-cadherin blotting was performed on the same membrane. Phospho-specific immunoblotting for FAK Y397 (pY397) or c-Src Y416 (pY416) phosphorylation was performed and the membranes were re-probed for total FAK or c-Src, respectively.

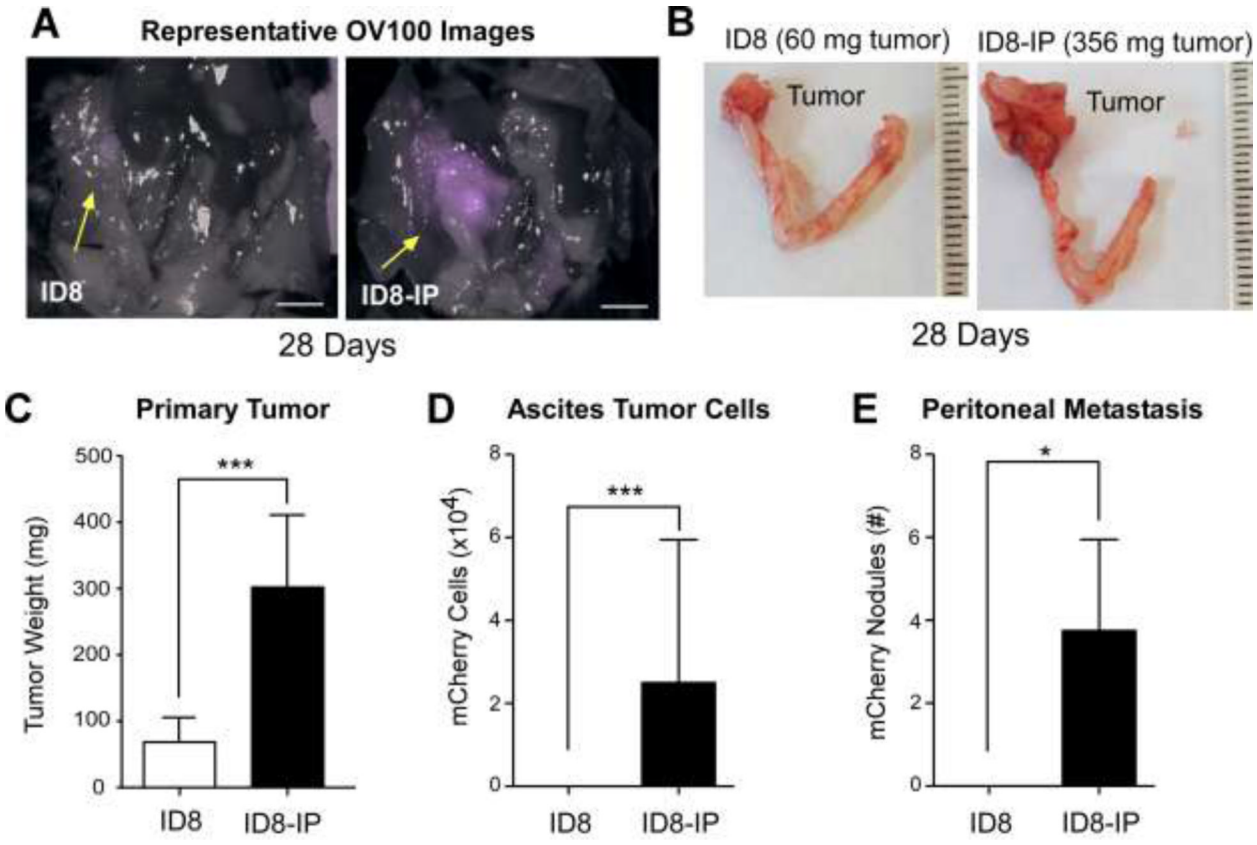

Figure 3.

ID8-IP ovarian carcinoma cells exhibit enhanced orthotopic tumor growth and metastasis. mCherry-expressing ID8 and ID8-IP cells (500,000 cells in 7 μL of Matrigel) were injected into the ovarian bursa of 8-10 week old C57Bl6 mice and evaluated after 28 days. (A) Representative images of combined mCherry-fluorescence with brightfield images of opened peritoneal cavity. Arrows (yellow) indicate positions of ovaries injected with ID8 or ID8-IP tumor cells. Scale is 0.5 cm. (B) Representative images of surgically extracted ID8 or ID8-IP ovarian tumors with uterine horns. Scale is 1 mm divisions. (C) Primary tumor weights of ID8 and ID8-IP injected mice. (D) Ascites was collected, peritoneal cavity washed with saline, and total mCherry-positive cells enumerated by flow cytometry. (E) Peritoneal-associated metastatic tumor sites were quantified by counting mCherry-positive nodules visualized by OV100 imaging. (C-E) Values are means (+/- SD) from ID8 (n=9) or ID8-IP (n=8) and represent one of two independent experiments (* $p<0.05$, *** $p<0.001$).

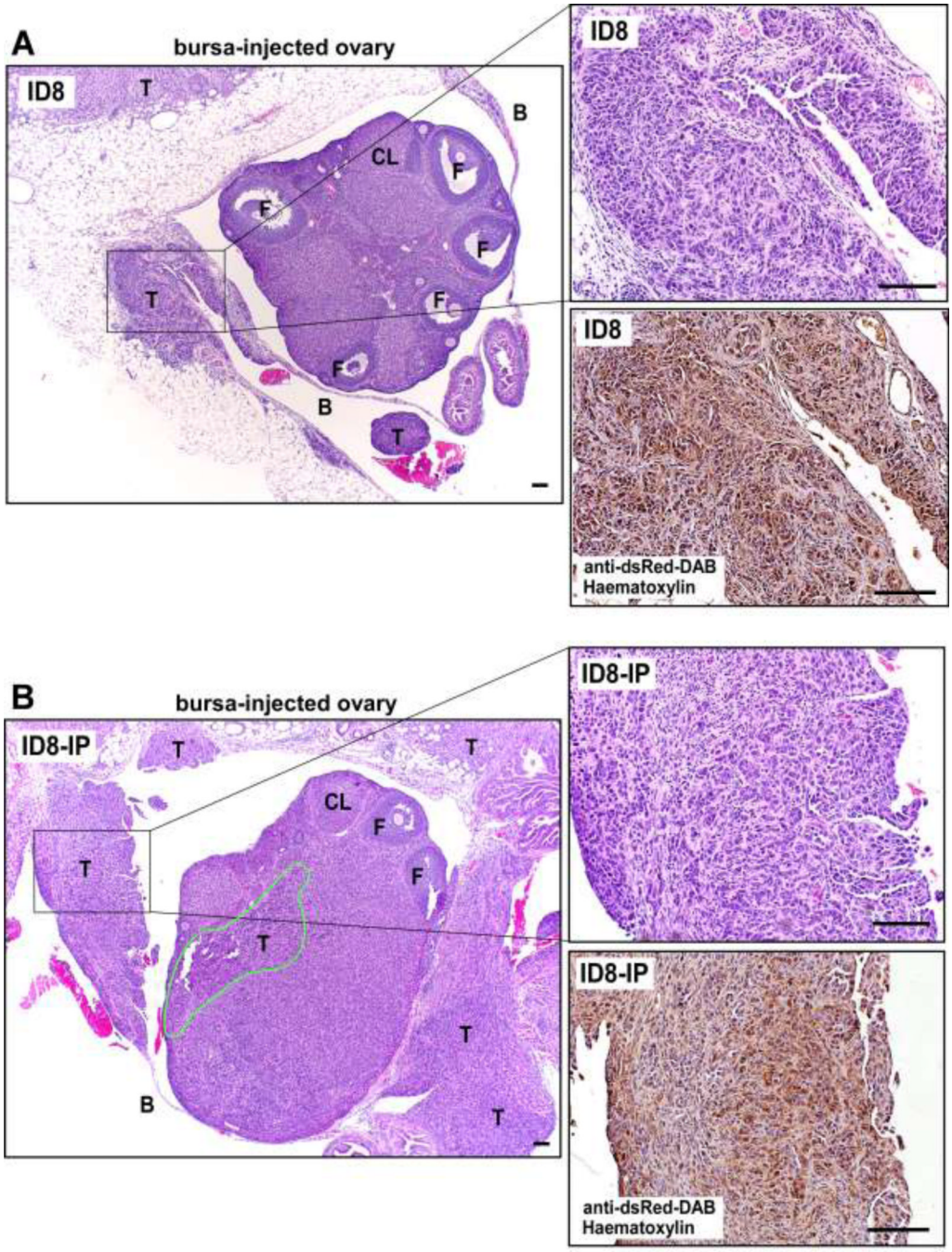

Figure 4.

Ovary-associated ID8 and ID8-IP tumors. (A) Representative x40 magnification of paraffin-embedded H&E-stained ID8 or (B) ID8-IP tumors 28 days after orthotopic injection. Right, is H&E x200 magnification (*boxed* region of x40 image) and a corresponding serial obtained tumor section stained with antibodies to dsRed (diaminobenzidine, DAB) and haematoxylin. The area of ID8-IP infiltration into the ovary is circled (green). The T, tumor; F, follicle, and CL, corpus luteum. Scale is 100 μm.

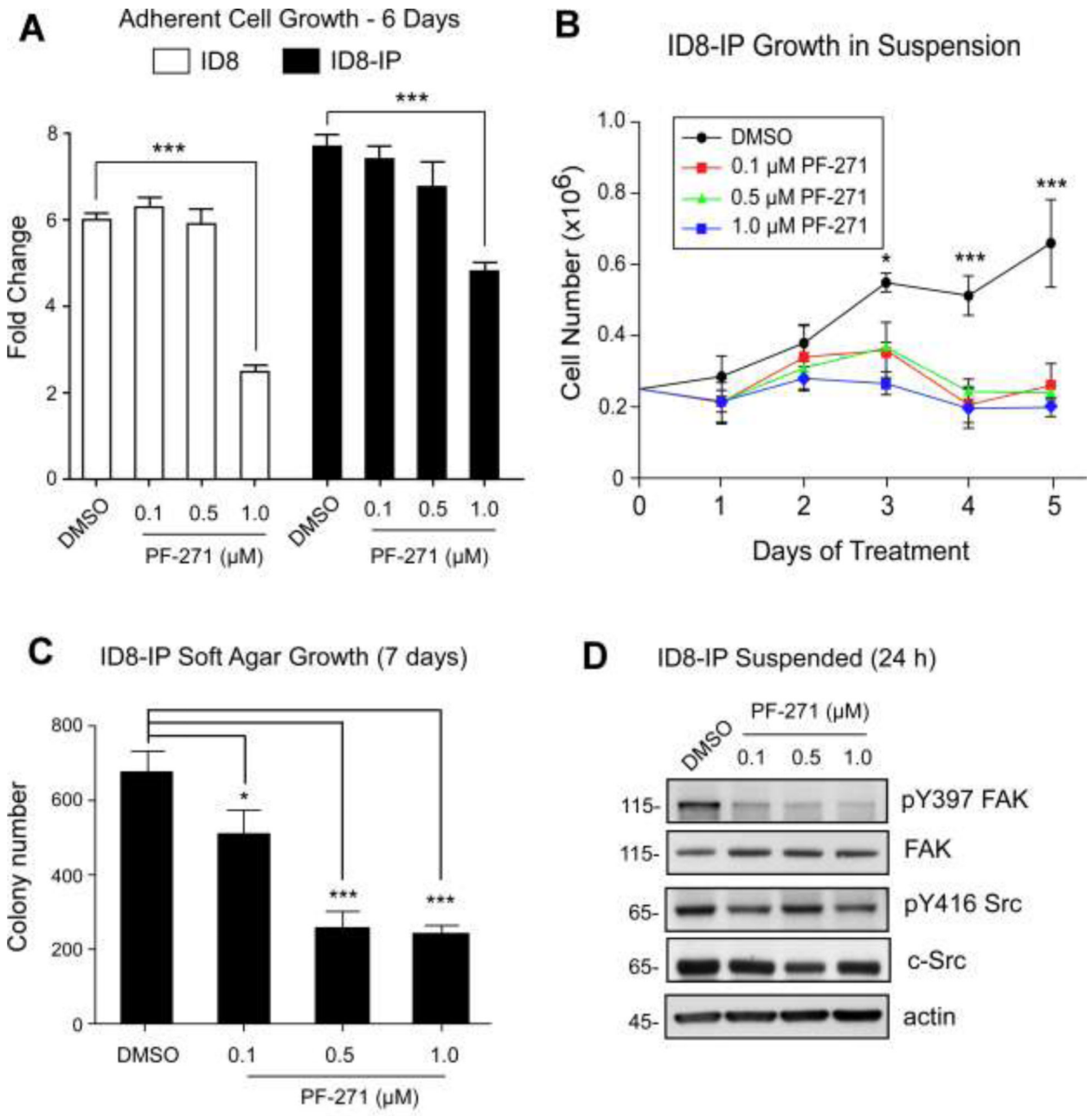

Figure 5.

PF-271 FAK inhibition prevents anchorage-independent ID8-IP growth without effects on c-Src Y416 phosphorylation. (A) Adherent proliferation of ID8 or ID8-IP cells over 6 days in the presence of vehicle (dimethylsulfoxide, DMSO) or increasing concentrations of PF-271 (0.1 to 1.0 μM). Values are average fold-change above 50,000 starting cells from triplicate points (+/- SD), (***p<0.001). (B) Anchorage-independent growth of 250,000 ID8-IP cells on poly-HEMA coated plates over 5 days in the presence of DMSO or increasing concentrations of PF-271 (0.1 to 1.0 μM). Values are means (+/- SD) of triplicate points, (*p<0.05, *** p<0.001). (C) ID8-IP soft agar colony number after 7 days in the presence of DMSO or increasing concentrations of PF-271 (0.1 to 1.0 μM). Values are means (+/- SD) of triplicate points, (*p<0.05, *** p<0.001). (D) Protein lysates of anchorage-independent

ID8-IP cells on poly-HEMA plates treated with DMSO or increasing concentrations of PF-271 (0.1 to 1.0 μM) were evaluated by immunoblotting for FAK Y397 phosphorylation (pY397), total FAK, c-Src Y416 phosphorylation (pY416 Src), total c-Src, and total actin levels.

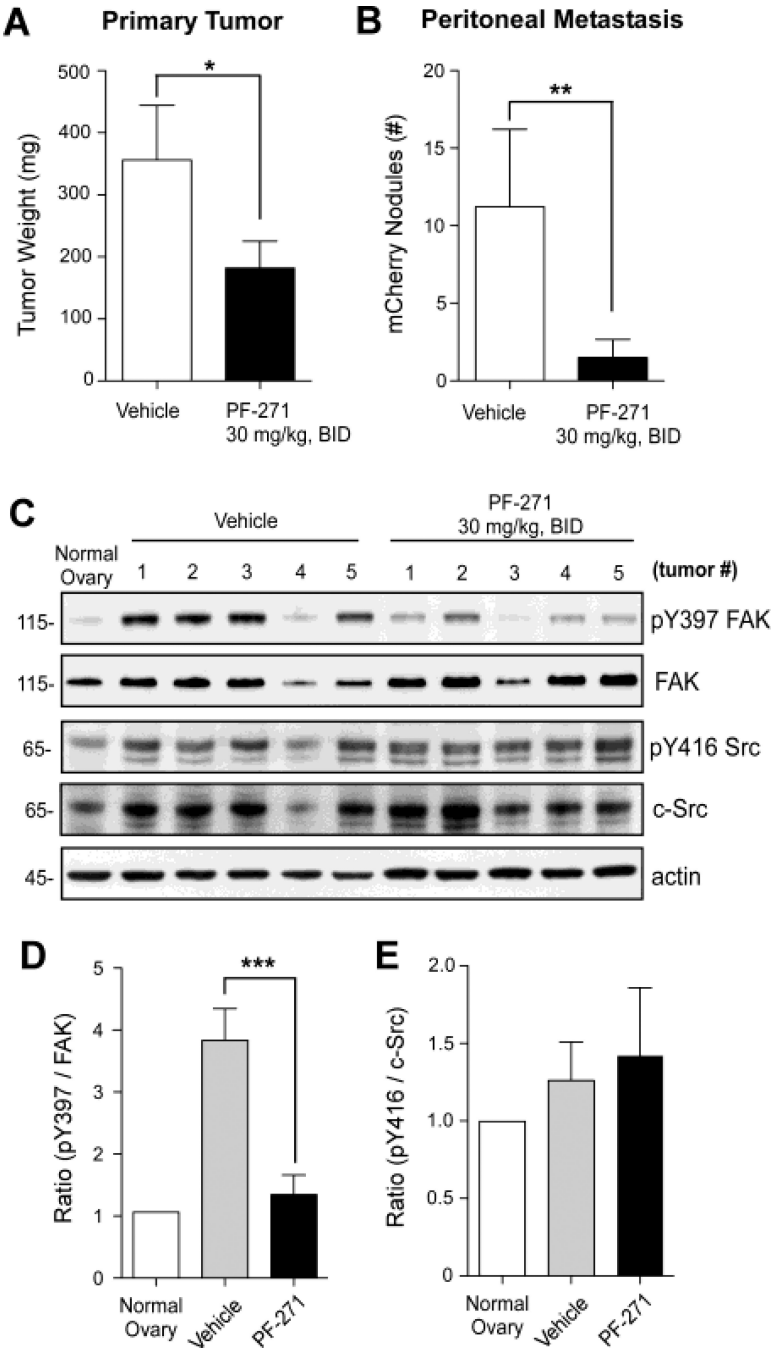

Figure 6.

Oral administration of PF-271 FAK inhibitor prevents ID8-IP tumor growth and metastasis independent of effects on c-Src Y416 phosphorylation. (A) mCherry-labeled ID8-IP tumor cells were bursal-injected and after 7 days, vehicle or PF-271 (30 mg/kg) were administered by oral gavage twice-daily (BID). Mice were euthanized after 28 days and (A) primary tumor weight was determined for mice treated with vehicle (n=8) or PF-271 (n=10). (B) Peritoneal-associated metastatic tumor sites were quantified by counting mCherry-positive nodules visualized by OV100 imaging. (A and B) Values are means (+/- SD) (* $p<0.05$, ** $p<0.01$). (C) Evaluation of FAK Y397 phosphorylation (pY397), total FAK, c-Src Y416 phosphorylation (pY416 Src), total c-Src, and total actin levels by immunoblotting using

normal ovary tissue or ID8-IP tumors from 5 independent vehicle- or PF-271-treated mice. (D) Ratio of pY397 phosphorylated FAK to total FAK levels normalized to normal ovary (set to 1) and determined by densitometry using Image J (n= 5 per group, *** $p<0.001$). (E) Ratio of pY416 phosphorylated c-Src to total c-Src levels normalized to normal ovary (set to 1) and determined by densitometry using Image J (n= 5 per group).

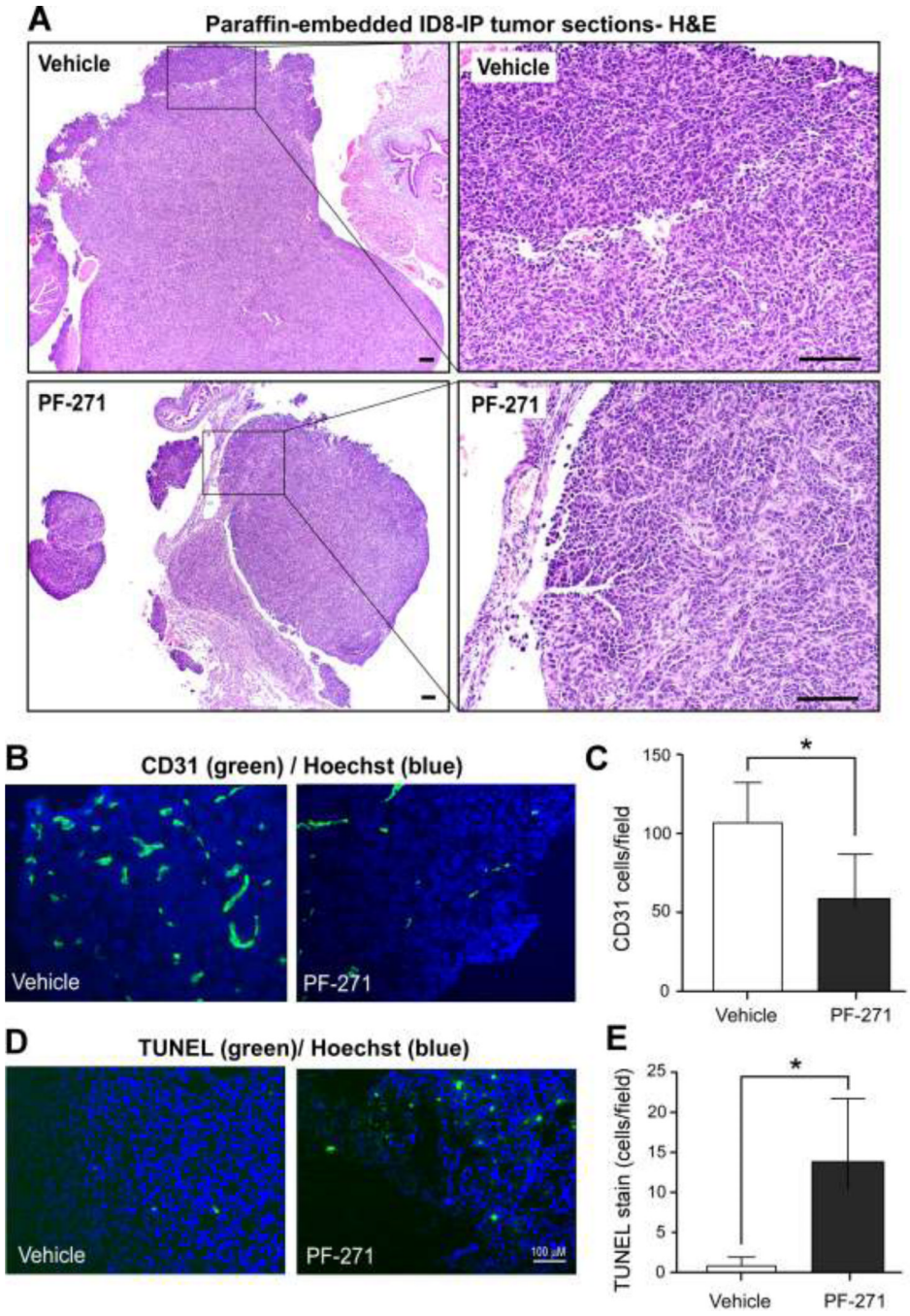

Figure 7.

Alterations in ID8-IP tumor-associated endothelial cells and tumor apoptosis in PF-271-treated mice. (A) Representative x40 images of paraffin-embedded H&E stained tumors from vehicle- or PF-271-treated mice. *Right*, boxed region x40 image at x200 magnification. Scale is 100 μM. (B) Representative fluorescent microscopy images of anti-CD31 antibody (green) and cell nuclei (Hoechst, blue) staining within ID8-IP tumors from vehicle- or PF-271-treated mice. (C) Fluorescent images from five random fields (at 10X) from 3 different ID8-IP tumors from vehicle- or PF-271-treated mice were acquired and the number of CD31-positive cells per field were enumerated using Image J. Values are means (+/- SD) (*$p<0.05$). (D) Representative fluorescent microscopy images of TUNEL (green) and cell

nuclei (Hoechst, blue) staining within ID8-IP tumors from vehicle- or PF-271-treated mice. Scale is 100 μM. (E) Images were acquired and enumerated as above. Values are means (+/- SD) (*p<0.05).

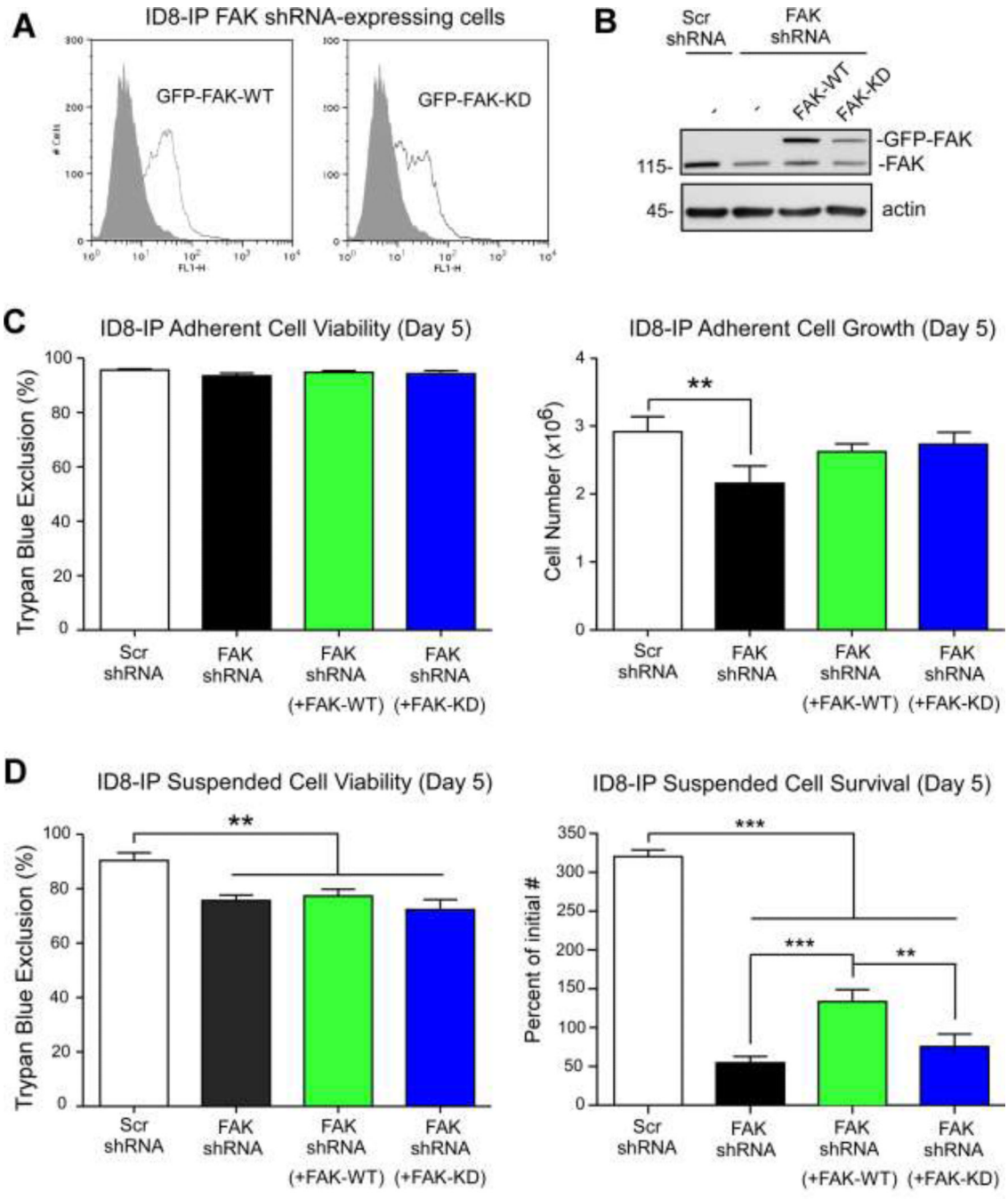

Figure 8.

Genetic support for the importance of FAK expression and activity in ID8-IP anchorage-independent cell survival. (A) Stable ID8-IP FAK shRNA knockdown cells were transiently reconstituted with GFP-FAK WT or GFP-FAK kinase-dead (KD), sorted for GFP-expression, and pooled populations of cells expanded and then used in cell proliferation assays within 10-14 days. Flow cytometry shows GFP (open histogram) or background cell fluorescence (dark histogram) of GFP-FAK WT and GFP-FAK KD cells after expansion. (B) Immunoblotting of ID8-IP cells lysates from scrambled shRNA (Scr), FAK shRNA-expressing, and FAK shRNA-expressing reconstituted with GFPFAK WT or GFP-FAK KD using antibodies to FAK and actin as a loading control. GFPFAK (150 kDa) and endogenous

FAK (115 kDa) are denoted. (C) Adherent cell viability and proliferation of 50,000 ID8-IP cells (Day 0) expressing Scr shRNA, FAK shRNA, and FAK shRNA cells reconstituted with GFP-FAK WT or GFP-FAK KD over 5 days as measured by ViCellXR enumeration. Values are means (+/- SD) of triplicate points (**$p<0.01$). (D) Suspended cell viability and survival of 250,000 ID8-IP cells (Day 0) expressing Scr shRNA, FAK shRNA, and FAK shRNA cells reconstituted with GFP-FAK WT or GFP-FAK KD over 5 days as measured by ViCellXR enumeration. Values are means (+/- SD) of triplicate points plotted as percent of initial cell number (**$p<0.01$, ***$p<0.001$).